International Journal of Nanomedicine

Dovepress
Taylor & Francis Group

Open Access Full Text Article

ORIGINAL RESEARCH

Highly Active and Stable Au@Pt Nanozymes-Based Colorimetric Nucleic Acids Detection for Varicella-Zoster Virus Diagnosis

Mingji Zong[1,*], Fengshou Liu[1,*], Lin Long[2], Jianbo Liu[1], Xiaochun Wu[3]

[1]College of Opto-Electronic Engineering, Zaozhuang University, Zaozhuang, People's Republic of China; [2]Zaozhuang Municipal Center for Disease Control and Prevention, Zaozhuang, People's Republic of China; [3]CAS Key Laboratory of Standardization and Measurement for Nanotechnology, National Center for Nanoscience and Technology, Beijing, People's Republic of China

*These authors contributed equally to this work

Correspondence: Lin Long, Zaozhuang Municipal Center for Disease Control and Prevention, Zaozhuang, People's Republic of China, Email zzcdcll@163.com; Jianbo Liu, College of Opto-electronic Engineering, Zaozhuang University, Zaozhuang, People's Republic of China, Email linyibm@163.com

Purpose: Currently, DNA is primarily detected using real-time quantitative polymerase chain reaction (qPCR) kits. However, their widespread clinical application is hindered by their high cost and the need for sophisticated instrumentation. Consequently, there is an urgent need to develop simpler DNA screening methods that are both cost-effective and compatible with resource-limited settings, thereby eliminating the need for complex equipment.

Methods: Taking advantage of the DNA-controlled property as well as the ultrahigh peroxidase-like catalytic activity of the Au@Pt nanozymes, we developed a simple and sensitive platform for the colorimetric detection of DNA sequence of varicella-zoster virus.

Results: Visual inspection of chromogenic reactions clearly demonstrated that the target DNA effectively inhibited the peroxidase-like activity of Au@Pt nanozymes. The response ranging from 1 to 1000 ng/mL, combined with a detection limit of 1ng/mL confirms the remarkable sensitivity of DNA-mediated regulation of Au@Pt nanozyme activity. Specificity assessment against other common infectious viruses revealed exceptional selectivity of the Au@Pt nanozyme system for varicella-zoster viruses. Moreover, the robust stability (retaining functionality for four weeks) of Au@Pt nanozymes further enhanced their practical utility.

Conclusion: This novel technology demonstrates high specificity for target DNA and achieved perfect agreement with RT-PCR in clinical validation. Its combination of operational simplicity, requiring no instrumentation, and remarkable stability positions it as a highly promising tool for diagnosing infectious diseases.

Keywords: nanozyme, core/shell nanostructures, nucleic acid detection, varicella-zoster virus, diagnosis

Introduction

Varicella, caused by the varicella-zoster virus (VZV), is an acute and highly contagious respiratory disease.[1] The virus exhibits high transmissibility and can infect multiple tissues in the human body, including the skin, nerves, and lymphocytes.[2] Consequently, establishing rapid and sensitive detection methods for VZV is crucial for effective outbreak prevention and control. PCR-based methods demonstrate particularly high sensitivity and specificity for detecting VZV nucleic acids across various clinical specimens.[3] Nevertheless, the requirement for specialized reagents (eg, fluorescent probes or DNA-binding dyes) and expensive instrumentation for fluorescence monitoring poses a significant barrier to the use of real-time PCR in point-of-care testing (POCT) environments.[4]

Nanozymes represent a novel class of artificial enzymes that combine the unique physicochemical properties of nanomaterials with intrinsic catalytic functionalities.[5–9] Compared with their natural counterparts, nanozymes exhibit superior characteristics, including enhanced stability, cost-effective mass production capability, and tunable enzymatic

Received: 3 September 2025
Accepted: 5 November 2025
Published: 8 November 2025

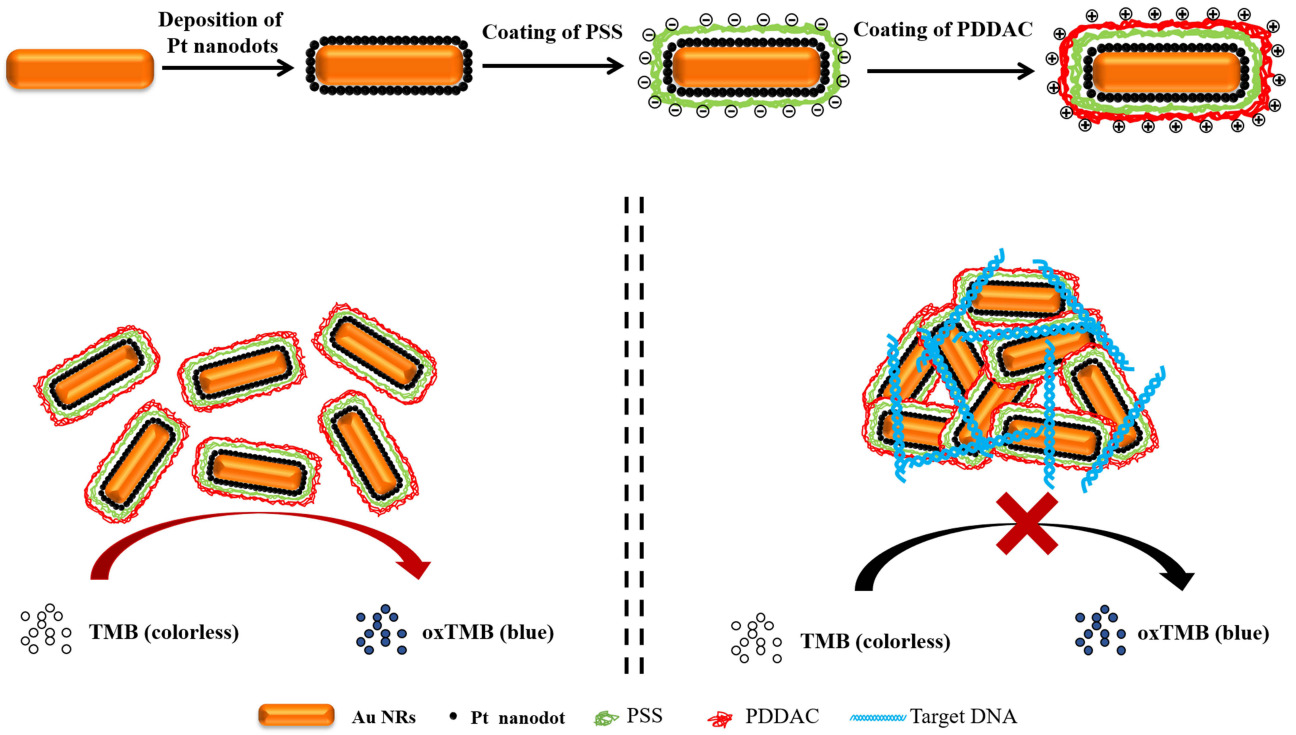

Scheme 1 Schematic representation of the synthetic procedure for Au@Pt nanozymes and the immunoassay of Au@Pt nanozymes based colorimetric platform.

activities.[10–14] Especially, noble metal-based nanozymes, which combine high stability, tunable enzyme-like activities, and excellent biocompatibility, drive significant advancements in biomedical applications in recent years.[15–19]

Label-free detection strategies have generated considerable interest because of their potential for rapid, cost-efficient, and equipment-free nucleic acid detection. To address this need, we developed a simple label-free colorimetric assay utilizing the peroxidase-mimicking activity of core-shell Au@Pt nanozymes for sensitive and visual diagnosis of VZV. The dual-layer polyelectrolyte-coated Au@Pt nanozyme nanorods exhibited excellent peroxidase-like activity and high stability, resulting in an efficient catalytic reaction of TMB with a clearly visible color change from blank to blue. The target DNA present in the solution directly caused a certain level of aggregation, leading to significant inhibition of substrate binding to the Au@Pt nanozymes required for peroxidase-like reactions. By shielding peroxidase activity in this way, PCR products reduce the rate of enzyme-catalyzed reactions. Unlike existing nucleic acid sensing methods, this method does not rely on fluorescence hybridization probes or fluorescent dyes, which are detected using complicated instrumentation. Instead, the detection of target nucleic acids is based on the fact that DNA amplification significantly inhibits the peroxidase-like activity of Au@Pt nanozymes. (Scheme 1).

Materials and Methods

Materials

Sodium borohydride ($NaBH_4$), cetyltrimethylammonium bromide(CTAB), l-ascorbic acid (AA), chloroauric acid ($HAuCl_4{\cdot}3H2O$), potassium tetrachloroplatinate(II) (K_2PtCl_4), silver nitrate (AgNO3), poly(styrene sulfonic acid) sodium salt (PSS), poly(diallyldimethylammonium chloride) (PDDAC), 30% H_2O_2, and 3,3',5,5'-tetramethylbenzidinedihydrochloride (TMB) were purchased from Alfa Aesar (USA) and used as received. The target DNA used in the current study and the PCR reagents were purchased from Shandong Acv Biotechnologies Co., Ltd. (China). The sequences used for PCR are presented in Table S1. Milli-Q water (18 MΩ cm) was used to prepare all solutions.

Synthesis of Gold Nanorods (Au NRs)

The Au NRs were synthesized using a seed-mediated growth procedure. CTAB-capped Au seeds were synthesized by chemical reduction of $HAuCl_4$ with $NaBH_4$. CTAB (0.1 M) (7.5 mL) was mixed with $HAuCl_4$ (100 μL, 24 mM), diluted to 9.4 mL, and magnetically stirred. Then, ice-cold $NaBH_4$ (0.6 mL, 0.01 M) was added. The color of the solution immediately changed from bright yellow to brown, indicating seed formation. Au seeds were used for 2–5 h. A 120 μL aliquot of the seed solution was added to a growth solution consisting of CTAB (100 mL, 0.1 M), $HAuCl_4$ (2.04 mL, 24 mM), $AgNO_3$ (1.05 mL, 10 mM), H_2SO_4 (2 mL, 0.5 M), and AA (800 μL, 0.1 M) to initiate the growth of Au NRs. The reaction was terminated after 12 h. The obtained Au NRs were purified by centrifuging the solution at 12000 rpm for 5 minutes. The precipitate was collected and redispersed in deionized water and the concentration of Au NRs was adjusted to 0.5 nM based on the rod molar extinction coefficient at 400 nm.

Synthesis of Au@Pt NRs

The Au@Pt NRs were prepared by overgrowth on the Au NRs following our previous reports. The purified Au NR solution (1 mL, 0.5 nM) was mixed with 50 μL of a 2 mM K_2PtCl_4 aqueous solution. Then, 10 μL of 0.1 M AA was added, and the total solution volume was diluted to 2 mL. The mixture was shaken vigorously and then placed in a 30 °C water bath for 30 min. Within several minutes, the color of the solution changed from pink to dark grey, suggesting the formation of a Pt shell. Then, 1 mL of 0.1 M CTAB was added.

Modification of the Au@Pt NRs with PSS

CTAB-coated nanorod solution (1 mL, 5 nM) was centrifuged at 12000 rpm for 10 min, and the precipitate was dispersed in 0.5 mL of PSS aqueous solution (2 mg/mL containing 6 mM NaCl). The resulting solution was stirred magnetically for 3 h. Subsequently, it was centrifuged at 12000 rpm for 10 min and the precipitate was redispersed in water.

Modification of the Au@Pt NRs with PDDAC

The PSS-coated nanorod solution (1mL, 5 nM) was dispersed in a 0.5 mL PDDAC aqueous solution (2 mg/mL containing 6 mM NaCl). The resulting solution was stirred magnetically for 3 h. Subsequently, it was centrifuged at 12000 rpm for 10 min and the precipitate was redispersed in water.

Peroxidase-Like Activity Analysis

To investigate the peroxidase-like activity of PSS-coated Au@Pt NRs and PDDAC-coated Au@Pt NRs, the catalytic oxidation of TMB in the presence of H_2O_2 was tested. For TMB as the substrate, the H_2O_2 concentration was fixed at 50 mM and the TMB concentration was fixed at 1 mM. Unless otherwise stated, the reaction was carried out at 37 °C in PBS buffer (0.1 M, pH 4.5) and used for absorption spectroscopic measurements at 650 nm. Catalytic parameters were determined by fitting the absorbance data to the Michaelis–Menten equation.

Au@Pt Nanozymes-Based Label-Free Colorimetric Assay

In a typical experiment, 20 μL of target DNA were mixed with 10 μL of Au@Pt nanozymes solution (5 nM) and then 1 mL of 0.1 M PBS (pH = 4.5), 10 μL of 100 mM TMB, and 50 μL of 1 M H_2O_2 were added to the mixture of Au@Pt nanozymes and target DNA. The mixed solution was incubated in a water bath at 37 °C for 5 min. For the detection of the target DNA, the reactions were terminated by adding a stop solution (100 μL of 10 M H_2SO_4). The absorption intensity was measured using a UV-visible spectrophotometer. Clinical oropharyngeal swabs were obtained from patients with clinical signs of varicella or those who had been exposed to varicella. Nucleic acids were extracted from clinical virus samples using a fast nucleic acid-releasing agent according to the manufacturer's instructions. The extracted nucleic acids were amplified by PCR to obtain a large number of target products, which were then detected using the Au@Pt nanozyme-based label-free colorimetric assay following the same procedures.

Characterizations

Ultraviolet-visible-near-infrared extinction spectra were obtained from a Varian Cary 60. Transmission electron microscopy was performed on Tecnai G2 T20 S-TWIN (T20). The zeta potential data were obtained from Delsa Nano C (Beckman Coulter, Brea, CA, USA).

Results and Discussion

Characterization of Au@Pt Nanozymes

We developed stable Au@Pt core-shell nanorods through template-guided growth and a layer-by-layer surface-modification strategy. As shown in Figure 1, Pt exhibited a Volmer-Weber growth mode on the Au nanorod substrates, forming a uniform coating of ~3 nm Pt nanodots that created well-defined core-shell structures. Optical characterization (Figure 2) revealed that the as-synthesized Au NRs exhibited characteristic longitudinal (730 nm) and transverse (510 nm) LSPR bands, which underwent significant redshifts to 800 and 520 nm, respectively, after Pt deposition at a Pt/Au ratio of 0.25. The longitudinal plasmon band showed particularly pronounced broadening and intensity damping following the Pt coating.

However, CTAB-capped Au@Pt NRs are unstable and tend to form aggregates in buffers or after the addition of chromogenic substrates.[20] To address this, we implemented an electrostatic layer-by-layer assembly approach using PSS and PDDAC polymers. Zeta potential measurements (Table 1) quantitatively tracked the surface charge evolution during stepwise modification of the nanorods. The as-synthesized Au NRs and Au@Pt NRs exhibited a positive zeta potential,

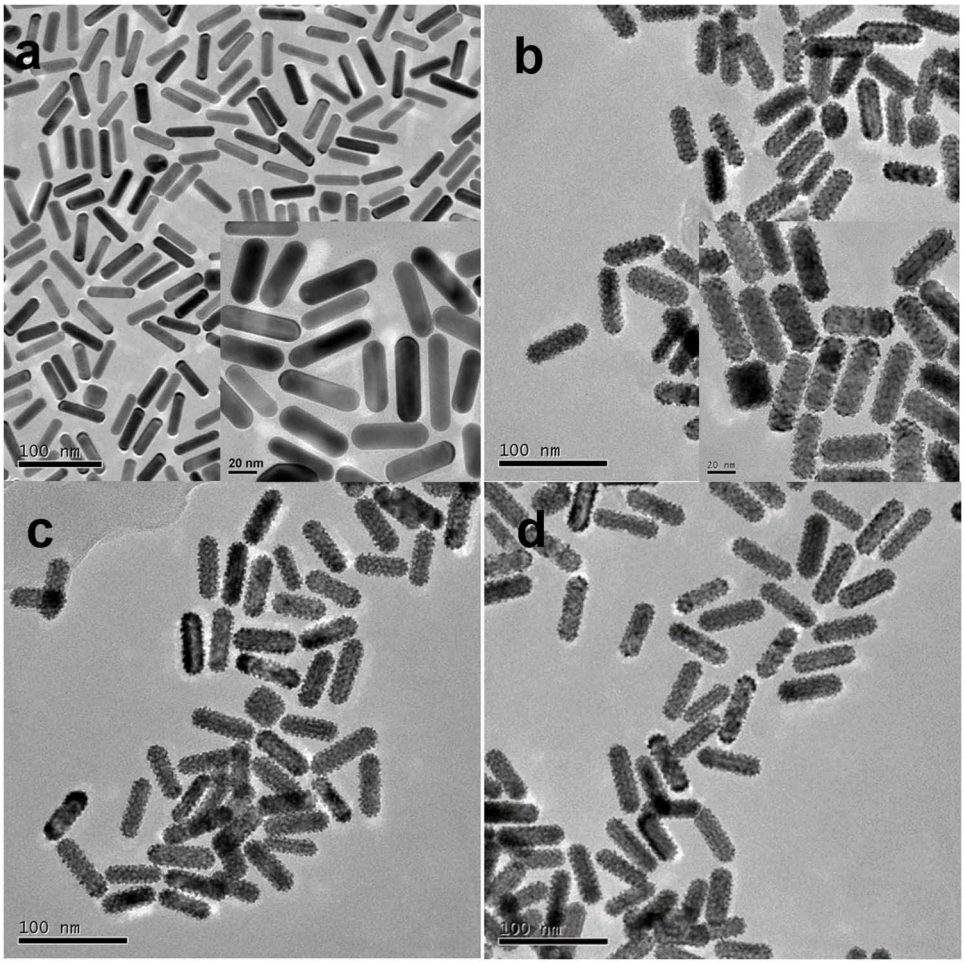

Figure 1 Typical TEM images of (**a**) Au NRs, (**b**) Au@Pt NRs, (**c**) PSS-coated Au@Pt NRs and (**d**) PDDAC-coated Au@Pt NRs. The insets show a high resolution scan for each sample.

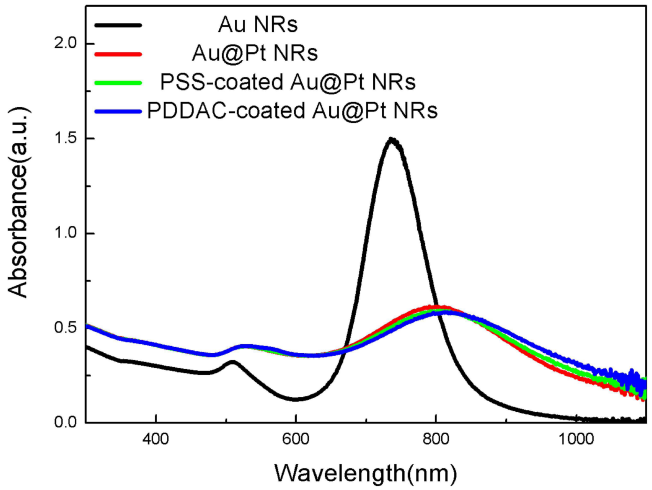

Figure 2 UV-vis-NIR spectra Au NRs, Au@Pt NRs, PSS-coated Au@Pt NRs and PDDAC-coated Au@Pt NRs.

which is characteristic of CTAB bilayer stabilization. Successful PSS adsorption was confirmed by charge reversal to −48.0 mV, indicating complete surface coverage by the anionic polymer. Subsequent PDDAC deposition restored the net positive surface charge (+37.5 mV), confirming the formation of a stable polyelectrolyte bilayer through electrostatic interactions. Both PSS- and PDDAC-coated samples maintained their original core-shell structures (Figure 1c and d). These observations, combined with zeta potential data, demonstrate that our electrostatic assembly process achieves stable surface functionalization without inducing particle aggregation or morphological changes.

DNA-Mediated Switch of Au@Pt Nanozymes Activity

TMB was used as a colorimetric probe to assess the peroxidase-mimicking capabilities of the nanozymes. The catalytic reaction induced a pronounced color transition as TMB was oxidized to its blue derivative (oxTMB), with a distinct absorption maximum at 650 nm. Notably, the nanozymes exhibited rapid catalytic kinetics, as evidenced by the immediate visual color change, clearly demonstrating their potent peroxidase-like activity (Figures 3,4).

Photographs of typical chromogenic substrates after catalytic oxidation by Au@Pt nanozymes showed that their peroxidase-like activity was inhibited by the target DNA (Figure 3). Quantitative analysis revealed a > 90% suppression of TMB oxidation in the presence of H_2O_2 when the target DNA was introduced (Figure 4). This dramatic inhibition suggests the rapid deactivation of nanozymes upon DNA exposure. In our case, the surface of the Au@Pt NRs was modified by negatively charged PSS and positively charged PDDAC; thus, deactivation may not be due to electrostatic interactions between DNA and the nanoparticle surface. Instead, inhibition primarily resulted from DNA-induced nanoparticle aggregation. This aggregation phenomenon effectively blocks the catalytic active sites and disrupts the peroxidase-mimicking function of nanozymes.

The catalytic performance of the PSS- and PDDAC-coated nanozymes was evaluated by determining their apparent enzyme kinetic parameters. As summarized in Table S2, the PDDAC-coated Au@Pt nanozymes are characterized by a higher V_{max}, indicating their enhanced catalytic activity. Building on these findings, our current results establish that PDDAC functionalization is essential for achieving high sensitivity in nanozyme-based detection systems. The cationic

Table 1 Zeta Potentials of Various Nanoparticles

Material	Zeta Potential(mV)
AuNRs	33.9±1.4
Au@Pt NRs	32.3±3.4
PSS-coated Au@Pt NRs	−48.0±2.7
PDDAC-coated Au@Pt NRs	37.5±0.6

https://doi.org/10.2147/IJN.S554033

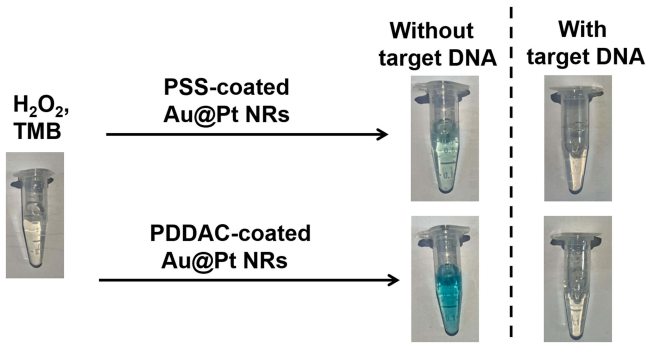

Figure 3 Photographs of typical chromogenic substrates after catalytic oxidation by Au@Pt nanozymes in the presence of target DNA and absence of target DNA. Reaction conditions: 0.05 nM Au@Pt NRs, 1 mM TMB, 50 mM H_2O_2, 5 minutes, 37°C, and 0.1 M, pH 4.5 PBS buffer.

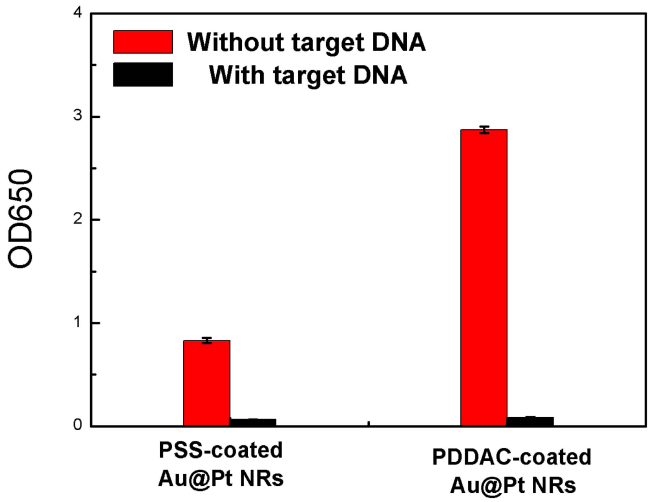

Figure 4 Effects of PSS coating and PDDAC coating on the performance of Au@Pt nanozyme based colorimetric platform. All the error bars were calculated based on the standard deviation of three measurements. Reaction conditions: 0.05 nM Au@Pt NRs, 1 mM TMB, 50 mM H_2O_2, 10 minutes, 37°C, and 0.1 M, pH 4.5 PBS buffer.

polymer coating synergistically improved colloidal stability and interfacial properties, resulting in superior catalytic performance.

Long-Term Stability Assessment of Au@Pt Nanozymes for Biosensing Applications

The development of highly stable catalysts with extended shelf lives is crucial for practical biosensor applications. To evaluate the storage stability of our Au@Pt nanozymes, we conducted a systematic four-week stability study at 4 °C. Remarkably, the nanozymes maintained their initial catalytic activity without any significant degradation throughout the observation period (Figure 5). To thoroughly assess the colloidal stability of the Au@Pt nanozymes, we systematically monitored both the effective diameter and zeta potential (Figure 6) over a four-week storage period. The nanozymes maintained consistent values for both parameters throughout the evaluation period, with no significant changes in the particle size distribution or surface charge characteristics. These results, combined with the sustained catalytic activity demonstrated in Figure 5, provide compelling evidence for the exceptional long-term stability of the Au@Pt nanozymes. The dual-layer polyelectrolyte coating provides greater stability than "bare" nanozymes while preserving the catalytic activity required for detection. This exceptional long-term stability demonstrates that Au@Pt nanozymes can be conveniently stored while retaining full functionality, making them particularly suitable for diagnostic applications that require reliable, ready-to-use catalytic components.

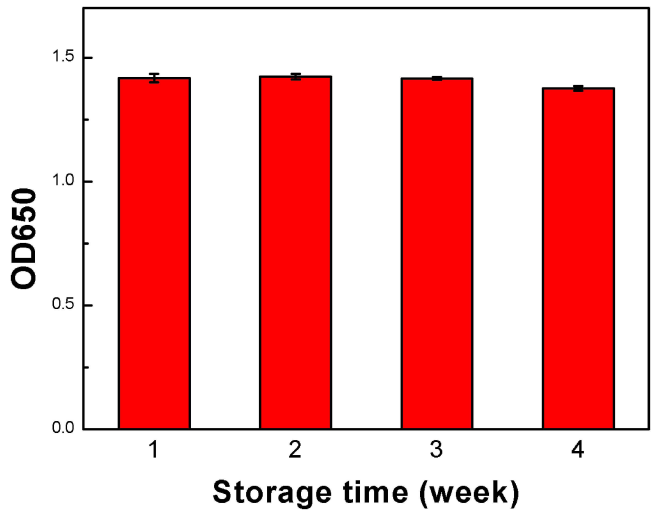

Figure 5 Effects of storage time on the reactivity of Au@Pt nanozymes at 4 °C. All the error bars were calculated based on the standard deviation of three measurements. 0.05 nM Au@Pt nanozymes, 1 mM TMB, 50 mM H_2O_2, 5 minutes, 37°C, and 0.1 M, pH 4.5 PBS buffer.

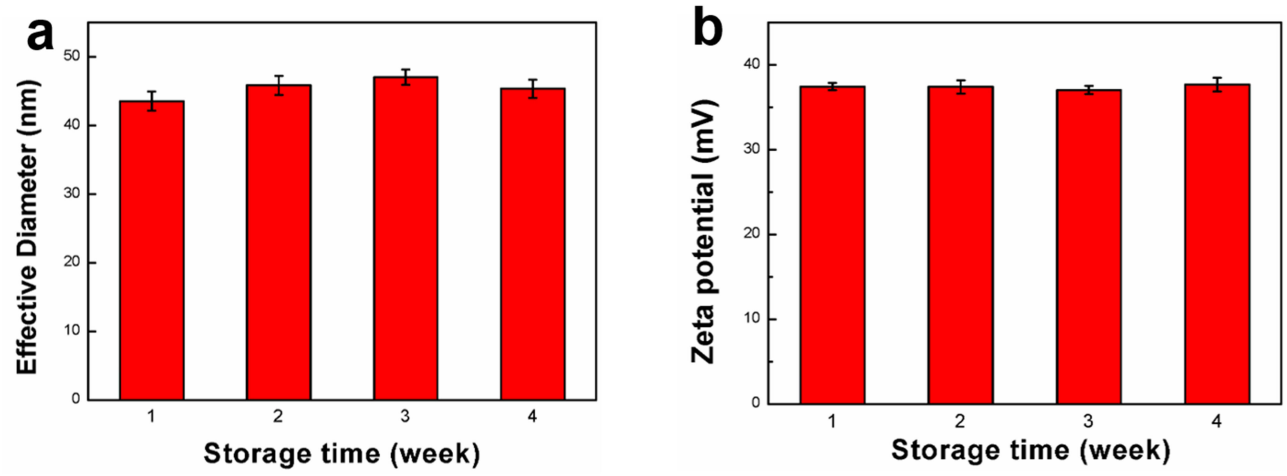

Figure 6 Effects of storage time on the stability of Au@Pt nanozymes from the viewpoints of effective diameter (**a**) and Zeta potential (**b**) in 0.1 M PBS solution (pH = 7.4) at 4 °C. All the error bars were calculated based on the standard deviation of three measurements.

Colorimetric Detection of Target DNA Using Au@Pt Nanozymes

Building on these findings, we further evaluated the quantitative detection capability of the Au@Pt nanozyme-based colorimetric assay for the target DNA. By synergistically combining the DNA-responsive modulation characteristics with the exceptional peroxidase-mimicking activity of Au@Pt nanozymes, we successfully established a highly sensitive colorimetric biosensor for sequence-specific DNA detection (Scheme 1). This innovative approach capitalizes on distinct visual signal changes mediated by target-DNA-induced nanozyme regulation, enabling rapid and equipment-free nucleic acid analysis. Figure 7 shows the concentration-dependent response of our detection system under optimized conditions, demonstrating effective DNA quantification through nanozyme inhibition. The results revealed distinct absorbance profiles at 450 nm across a broad detection range (0–1000 ng/mL), with the system achieving a detection limit of 1 ng/mL. The high analytical sensitivity could contribute to a reduction in false negatives during the early stages of viral infection screening. Furthermore, the system exhibited a good linear correlation between absorbance variation and DNA concentration in the 0–10ng/mL range (Figure 7). This linear response, combined with the ultra-low detection limit, confirms the remarkable sensitivity of DNA-mediated regulation of Au@Pt nanozyme activity. Such predictable and

https://doi.org/10.2147/IJN.S554033

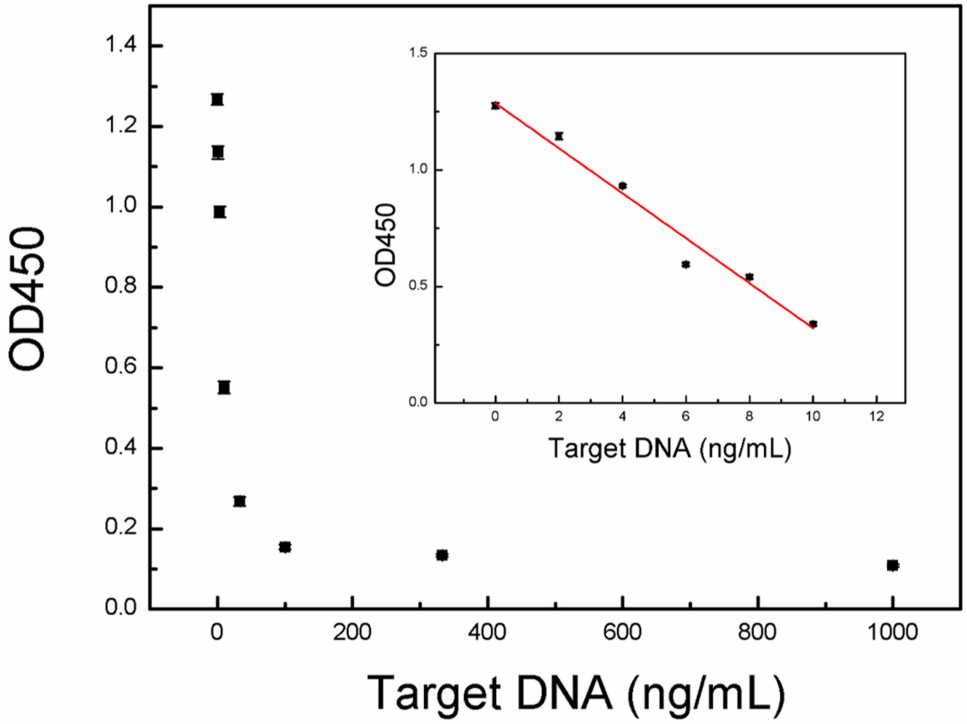

Figure 7 The absorbance at 450nm of Au@Pt nanozymes based colorimetric platform varies with the concentration of target DNA. Inset: linear calibration plot for target DNA. All error bars were calculated based on the standard deviation of three measurements.

reproducible dose-response characteristics demonstrate the suitability of the platform for precise nucleic acid diagnosis in clinical and research applications.

Application of Biomedical Assay VZV Detection in Clinical Samples

As shown in the graph in Figure 3, an obvious reduction in the colorimetric signal was observed using the Au@Pt nanozyme system. The reduced color intensity associated with the target DNA was easily distinguished from that of the negative control by the naked eye. A real sample analysis was conducted using clinical oropharyngeal swabs to verify the practical applicability of our approach. In a clinical evaluation of 50 specimens, our Au@Pt nanozyme-based colorimetric assay achieved perfect diagnostic agreement with reference RT-PCR results (Table 2). These results validate the clinical applicability of the Au@Pt nanozyme-based colorimetric platform.

The specificity of the Au@Pt nanozyme-based system for VZV diagnosis was also investigated by comparing it with other infectious viruses, such as measles virus (MV), rubella virus (RV) and mumps virus (MUV). As shown in Figure 8, very weak signals were acquired only for the VZV-positive sample. Stronger optical densities were observed for other positive and negative samples. The results demonstrated that the VZV nucleic acid can be effectively recognized by the proposed Au@Pt nanozyme-based system with high specificity.

Table 2 Comparison of Assay Performance of Au@Pt Nanozyme Based Colorimetric Assay and RT-PCR for Clinical Samples

Assay	Total	Positive	Negative
Au@Pt nanozyme based colorimetric assay	50	28	22
RT-PCR	50	28	22

Notes: ΔOD450 is the difference between the absorbance of the negative control and specimen. A positive result was defined as any ΔOD450 greater than three times the standard deviation (SD) of the negative control, which was determined by RT-PCR analysis of a panel of 10 negative samples for VZV.

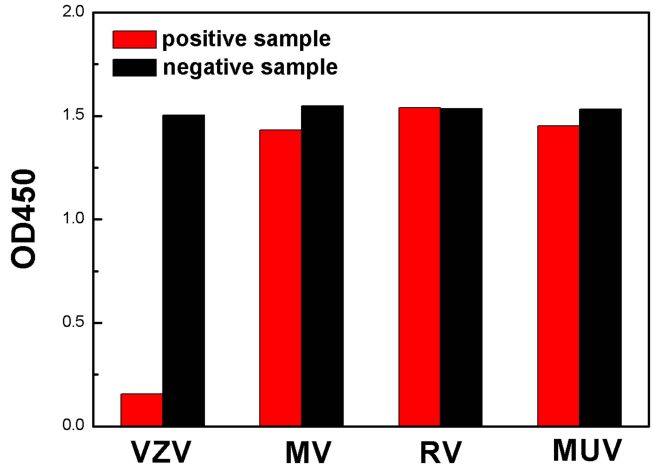

Figure 8 Specifity of the Au@Pt nanozymes based system for VZV diagnosis.

Conclusion

In this study, we developed a simple colorimetric DNA detection method utilizing Au@Pt nanozymes that enabled rapid visual detection with a detection limit of 1 ng/mL. The system demonstrated excellent specificity for target DNA sequences and 100% concordance with RT-PCR for clinical sample validation. A dual-layer polyelectrolyte coating was developed for the nanozyme, ensuring high stability while maintaining high catalytic activity, offering a significant advantage for clinical detection, particularly in the field of infectious disease diagnosis. Although the current Au@Pt nanozyme-based system has not been applied in more complex environments, this strategy provides valuable insights for future nanozyme-based detection platforms with improved diagnostic performance, guiding optimization efforts such as more sophisticated surface modifications and a thorough mechanistic investigation.

Ethics Approval and Informed Consent

All experiments were approved by the Ethics Committee of Zaozhuang University (Approval No. EC2025-0015) and conducted in accordance with the Zaozhuang Disease Control and Prevention Laboratory Ethics Guidelines. Consent for participation was not applicable. This study was conducted in accordance with the principles of the Declaration of Helsinki.

Funding

This study was financially supported by the International Cooperation Program of Shandong Provincial Government of 2023 by the Ministry of Education of Shandong Province, China and Natural Science Foundation of Shandong Province, China (grant no. ZR2020MB068).

Disclosure

The authors report no conflicts of interest in this work.

References

1. Heininger U, Seward JF. Varicella. *The Lancet*. 2006;368:1365–1376.
2. Gershon AA, Breuer J, Cohen JI, et al. Varicella zoster virus infection. *Nat Rev Dis Primers*. 2015;1(1):1–18. doi:10.1038/nrdp.2015.16
3. Gershon AA, Silverstein SJ. Varicella zoster virus. *Clin Virol*. 2009;451–474.
4. Leung J, Harpaz R, Baughman AL, et al. Evaluation of laboratory methods for diagnosis of varicella. *Clin Infect Dis*. 2010;51(1):23–32. doi:10.1086/653113
5. Liang M, Yan X. Nanozymes: from new concepts, mechanisms, and standards to applications. *Acc Chem Res*. 2019;52(8):2190–2200. doi:10.1021/acs.accounts.9b00140
6. Zandieh M, Liu J. Nanozymes: definition, activity, and mechanisms. *Adv Mater*. 2024;36(10):2211041. doi:10.1002/adma.202211041
7. Wang H, Wan K, Shi X. Recent advances in nanozyme research. *Adv Mater*. 2019;31(45):1805368. doi:10.1002/adma.201805368

8. Liu Q, Zhang A, Wang R, et al. A review on metal-and metal oxide-based nanozymes: properties, mechanisms, and applications. *Nano-Micro Letters*. 2021;13(1):154. doi:10.1007/s40820-021-00674-8
9. Yang W, Yang X, Zhu L, et al. Nanozymes: activity origin, catalytic mechanism, and biological application. *Coordin Chem Rev*. 2021;448 (1):214170. doi:10.1016/j.ccr.2021.214170
10. Chen Z, Yu Y, Gao Y, et al. Rational design strategies for nanozymes. *ACS Nano*. 2023;17(14):13062–13080. doi:10.1021/acsnano.3c04378
11. Tang G, He J, Liu J, et al. Nanozyme for tumor therapy: surface modification matters. *Exploration*. 2021;1(1):75–89. doi:10.1002/EXP.20210005
12. Chang Y, Gao S, Liu M, et al. Designing signal-on sensors by regulating nanozyme activity. *Analyt Meth*. 2020;12(39):4708–4723. doi:10.1039/D0AY01625J
13. Wang Q, Wei H, Zhang Z, et al. Nanozyme: an emerging alternative to natural enzyme for biosensing and immunoassay. *TrAC Trends Analyt Chem*. 2018;105:218–224. doi:10.1016/j.trac.2018.05.012
14. Zhang R, Jiang B, Fan K, et al. Designing nanozymes for in vivo applications. *Nat Rev Bioengine*. 2024;2:849–868.
15. Jiang D, Ni D, Rosenkrans ZT, et al. Nanozyme: new horizons for responsive biomedical applications. *Chem Soc Rev*. 2019;48(14):3683–3704. doi:10.1039/C8CS00718G
16. Cai E, Qi X, Shi Y, et al. Immunomodulatory melanin@ Pt nanoparticle-reinforced adhesive hydrogels for healing diabetic oral ulcers. *Chem Engine J*. 2024;488:150372. doi:10.1016/j.cej.2024.150372
17. Zhang Y, Wei G, Liu W, et al. Nanozymes for nanohealthcare. *Nat Rev Meth Primers*. 2024;4(1):36. doi:10.1038/s43586-024-00315-5
18. Qi X, Cai E, Xiang Y, et al. An immunomodulatory hydrogel by hyperthermia-assisted self-cascade glucose depletion and ROS scavenging for diabetic foot ulcer wound therapeutics. *Adv Mater*. 2023;35(48):2306632. doi:10.1002/adma.202306632
19. Zhang T, Tian F, Long L, et al. Diagnosis of rubella virus using antigen-conjugated Au@ Pt nanorods as nanozyme probe. *Inter J Nanomed*. 2018;13:4795–4805. doi:10.2147/IJN.S171429
20. Liu J, Hu X, Hou S, et al. Au@ Pt core/shell nanorods with peroxidase-and ascorbate oxidase-like activities for improved detection of glucose. *Sensors Actuators B*. 2012;166:708–714. doi:10.1016/j.snb.2012.03.045